Vehicle-to-Vehicle IEEE 802.11p performance measurements at urban intersections

Conference Paper · June 2012

DOI: 10.1109/ICC.2012.6364714

7 authors, including:

Henrik Schumacher
Leibniz Universität Hannover

Tchouankem Hugues Narcisse
Leibniz Universität Hannover

Thomas Kürner
Technische Universität Braunschweig

Lars Wolf
Technische Universität Braunschweig

Vehicle-to-Vehicle IEEE 802.11p Performance Measurements at Urban Intersections

Henrik Schumacher*, Hugues Tchouankem*, Jörg Nuckelt†, Thomas Kürner†,
Tetiana Zinchenko‡, André Leschke‡ and Lars Wolf§
*Institut für Kommunikationstechnik, Leibniz Universität Hannover, Hannover, Germany
†Institut für Nachrichtentechnik, Technische Universität Braunschweig, Braunschweig, Germany
‡Volkswagen AG, Wolfsburg, Germany
§Institut für Betriebssysteme und Rechnerverbund, Technische Universität Braunschweig, Braunschweig, Germany

***Abstract*—During the last few years, vehicle-to-vehicle (V2V) wireless communication has become a key objective for enabling future cooperative safety applications, such as intersection collision warning. In this paper, we present the results of a 5.9 GHz V2V performance measurement campaign at four different urban intersections under NLOS conditions using commercial off-the-shelf wireless interface cards which meet the 802.11p and ITS-G5 specifications. Particularly, we quantify the packet delivery ratio (PDR) and received signal strength indication (RSSI) levels associated with different scenario conditions with respect to vehicle positioning, intersection geometry and traffic density. We determine reliable communication ranges which constitute an important metric for V2V collision avoidance applications.**

I. Introduction

During the last years, V2V communication systems have become a key objective in prevalent discussions, being regarded as a further step towards increasing traffic safety and efficiency as well as facilitating the driving process.

For this reason, the IEEE 802.11p [1] standard has been developed, which is meant to provide the basis for Dedicated Short Range Communications (DSRC) in the 5.9 GHz frequency band. IEEE 802.11p is an approved amendment to the well-known IEEE 802.11 [2] standard introducing several modifications to adapt the physical (PHY) layer and Medium Access Control (MAC) sublayer to the requirements of highly dynamic vehicular environments. In particular, the 802.11p PHY layer is mainly based on IEEE 802.11a. In order to make the signal more robust against fading effects, 802.11p uses a channel bandwidth of 10 MHz instead of the usual 20 MHz. Furthermore, the MAC sublayer of IEEE 802.11p introduces several modifications; the most important one is the newly defined Outside the Context of a Basic Service Set (OCB) mode which allows stations to transmit data frames without prior association or authentication with a Basic Service Set (BSS). In Europe, the main characteristics of 802.11p have been adopted by ETSI ITS-G5 [3].

One of the main prerequisites for reliable and efficient operation of any V2V application is the quality of the communication link, which depends significantly on the characteristics of the radio channel. For enabling V2V applications, it is essential to perform a deep analysis of the fundamental wave propagation characteristics in typical vehicular environments.

Therefore, numerous measurement campaigns as well as simulation studies have been carried out recently. In [4], a survey of comprehensive V2V propagation channel measurement campaigns in different relevant environments is given. Authors in [5] also provide an overview of V2V radio channel measurements at 5.6 GHz and describe power delay profiles and the Doppler spectral density, especially focusing their research on most relevant scenarios for safety-related applications, but not on urban scenarios.

The most critical communication scenarios are considered to be in non-line-of-sight (NLOS) situations, being a characteristic pattern of any urban environment due to a dense grid of high buildings [6]. Here, the radio channel is very susceptible to multipath propagation and shadowing effects as two main characteristics of urban environments. While these effects can cause packet loss which may subsequently lead to incorrect safety-relevant information about the vehicle's surroundings, reliable communication in urban NLOS scenarios is an important prerequisite for certain cooperative safety applications, e. g., intersection collision warning.

Radio channel characterization in NLOS scenarios is in focus of only a few research groups, though. Basically, there are two different approaches: Karedal et al. [7] provide results from a profound measurement study of intersection scenarios using a channel sounder creating power delay profiles. These results cannot be applied directly to assess the performance of real 802.11 transceivers. For this reason, Mangel et al. [8] present an elaborate measurement study in urban environments using 802.11 interfaces. Our work contributes to the general analysis of urban intersections and covers additional issues like the impact of street width or traffic density.

For this purpose, we quantify RSSI levels, packet delivery ratios (PDRs), which reflect the ratio between the numbers of successfully received and transmitted frames, and reliable communication ranges associated with different intersection characteristics, such as building density and development, street and intersection width. Insights into these metrics are necessary to meet the requirements of reliable communication ranges for collision avoidance applications. The results are obtained by means of measurements in realistic V2V application scenarios using a measurement system that meets current standards for vehicular communications.

978-1-4577-2053-6/12/$31.00

The remainder of this paper is organized as follows: In Section II, we describe the setup of the measurement campaign carried out in different urban crossroad scenarios in the city of Braunschweig. Section III presents the obtained results in terms of PDRs, received power levels and reliable communication ranges. Finally, we conclude our work in Section IV.

II. Measurement Setup

A. Measurement Equipment

The test setup included two vehicles of similar height: A Volkswagen Scirocco III with a panorama glass roof was configured as transmitter and a Mercedes-Benz W202 C-Class operated as receiver. Fig. 1 depicts the hardware components that were used for the measurements. Each vehicle was equipped with a communication module which included an ALIX3D3 board running an Ubuntu Linux distribution with kernel version 2.6.32. We used commercial off-the-shelf Compex Mini PCI 802.11abg wireless cards based on the Atheros AR5006X (AR5414) chipset. The communication module was also equipped with a Navilock NL-402U Global Positioning System (GPS) receiver using the u-blox5 chipset in order to log the vehicle positions and the distance between the vehicles.

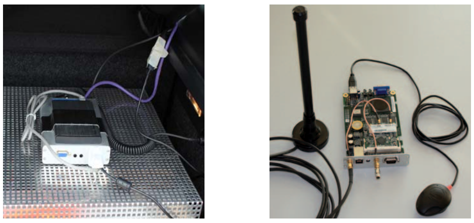

(a) (b)

Figure 1: The communication module inside the trunk of a vehicle (a) and a detailed view of the ALIX3D3 board with the GPS receiver and the magnetic mount antenna (b).

Furthermore, each vehicle was equipped with a vertically polarized magnetic mount antenna (Mobile Mark ECOM6-5500) mounted on its roof. The antennas have kindly been measured by Delphi Deutschland GmbH and show an omni-directional radiation pattern and a nominal antenna gain (including antenna cable attenuation) of 3.2 dBi at zero degrees elevation on a metal ground plane. The transmit and receive antenna heights were approximately 1.5 m. While the antenna was mounted at the center of the receiving vehicle's roof, we placed it a little further rearward on the transmitting vehicle due to its panorama glass roof (see Fig. 2).

The transmit power was configured to be 23 dBm. Together with the antenna gain and a system loss of approximately 3 dB caused by the connectors between interface card and external antenna, this resulted in an equivalent isotropically radiated power (EIRP) of 23.2 dBm.

In order to ensure applicability of the measurement results for prospective cooperative safety applications, the utilized wireless interfaces have to meet the IEEE 802.11p [1] or ITS-G5 [3] specifications. Hence, we used a modified driver based on ath5k and the Linux wireless subsystem. As a result, we are able to conduct tests on a 10 MHz channel centered at 5.9 GHz employing the OCB mode defined in 802.11p and adopted by ITS-G5. Furthermore, the driver supports radiotap header generation to gather measurement data.

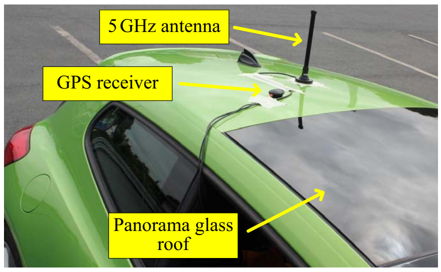

Figure 2: Antenna placement with a panorama glass roof.

On the transmitting node, a packet generator was configured to send periodic messages with a generation rate of 100 Hz and a net message size of 500 bytes. Including UDP, IP, LLC and MAC header (8/20/8/28 bytes), this resulted in a MAC frame size of 564 bytes. The receiving wireless interface remained in monitor mode, passively listening to frames on the configured channel. RSSI values were extracted from the radiotap header and recorded for each successfully received frame.

A self-developed software tool running at the receiver utilizing the *libpcap* library was used to log the measured RSSI values as well as the transmitter and receiver position for each frame reception. In order to compute the PDR, we used a 32-bit sequence number in the message payload. Additionally, several scripts were implemented to control the experiments during the measurements and adapt the parameter settings based on predefined configuration files. A summary of the measurement system parameters is presented in Table I.

Transmission power (EIRP)	23.2 dBm
Center carrier frequency	5.9 GHz
Channel bandwidth	10 MHz
Data rate	6 Mbps
Antenna height	1.5 m
Packet generation rate	100 Hz
MAC frame / message payload size	564 / 500 Bytes

Table I: Measurement system parameters.

In [9], the authors analyze the impact of a large panorama glass roof based on 5.9 GHz measurements conducted in an anechoic chamber. Their results indicate that a gain reduction of 15 to 20 dB can be caused by this roof type, which the authors attribute to waveguide effects. Motivated by these results, we conducted a preliminary test involving the two test vehicles, one of them also equipped with a panorama glass roof (see Fig. 2), which, however, was considerably smaller than the one tested in [9]. We performed this test under perfect line-of-sight (LOS) conditions, moving the receiver around the transmitter while keeping the distance between both unchanged. The obtained results showed no noticeable influence of the glass roof. Additional measurements revealing an omnidirectional antenna pattern confirmed these observations. We attribute this to the exposed antenna position and the fact that the test vehicle's glass roof was significantly smaller.

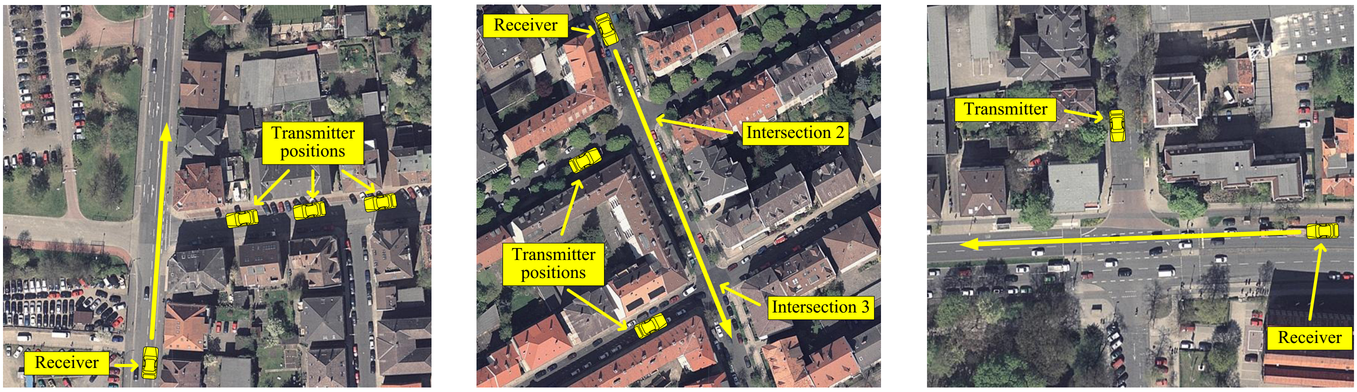

(a) Intersection 1: Varying transmitter positions. 52°16'36.61"N, 10°31'33.19"E.

(b) Intersections 2 and 3: Varying street width. 52°16'21.60"N, 10°32'25.35"E (Int. 3) and 52°16'19.43"N, 10°32'27.01"E (Int. 4).

(c) Intersection 4: Large intersection, dense traffic. 52°16'31.76"N, 10°31'42.75"E.

Figure 3: Selected scenarios: Arrows indicate the direction of motion of the receiving vehicle. The transmitting vehicle's position is fixed for each of the 6 scenarios. Geographic coordinates of each intersection's center are given.

B. Measurement Scenarios

The measurement campaign was carried out in the city of Braunschweig at selected intersections with different traffic conditions. In order to quantify the effects of buildings, traffic and the topology of the intersections, we selected 9 different scenarios at 6 different intersections in an urban environment. In this paper, we present the results for 6 of these scenarios at 4 different intersections (see Fig. 3). All scenarios have in common that the transmitter was located at a fixed position on a side street, while the receiving vehicle moved towards the intersection with a speed of approximately 20-25 km/h.

Intersection 1: The objective of the first three scenarios is the evaluation of the influence of the transmitter's position. Hence, all of these scenarios were located at intersection 1 (Mittelweg - Nordstrasse), where we varied the transmitter's distance d_{TX} to the intersection center between 35, 55 and 85 m. The intersection is half-open, which means that there are buildings on two intersection quadrants only, although there were several parked vehicles opposite to the buildings. The intersection is of medium width with a distance of approximately 13 m between the intersection center and the corners of the buildings and a width of the side street, where the transmitter was located, of approximately 16 m. The traffic density was very low.

Intersections 2 and 3: The scenarios at intersections 2 (Waterloostrasse - Schunterstrasse) and 3 (Waterloostrasse - Wabestrasse), which are similar to the "narrow urban" intersection type in [7], consider the influence of the intersection and street width. The structure of the surrounding buildings is quite similar in both scenarios. The main difference is related to the width of the streets where the transmitter was located. In the Schunterstrasse (intersection 2), the width of the building canyon is approximately 20 m (which makes this intersection approximately comparable to the "urban main case" in [8]), whereas the Wabestrasse (intersection 3) offers a width of only 10 m. Furthermore, there were several leaved trees in the Schunterstrasse, while the Wabestrasse showed almost no vegetation. In both cases, the distance between transmitter and intersection center was $d_{TX} = 25\,\mathrm{m}$. Traffic density was very low during the measurements.

Intersection 4: The sixth and last scenario was located at intersection 4 (Rebenring - Geysostrasse), a wide intersection with a distance between the intersection center and the corner of the nearest building of approximately 21 m. There are buildings on three intersection quadrants, and the buildings in the side street, where the transmitter was positioned, are located relatively close to the street. On the main street (Rebenring), there are two lanes per direction, in contrast to all other streets being part of the selected scenarios. The distance between transmitter and intersection center was $d_{TX} = 45\,\mathrm{m}$. In contrast to the other scenarios, the traffic density was very high, with vehicles often stopping at the traffic lights and occasional appearance of buses.

III. Measurements Results

In this section, the results from the measurement campaign are presented. Prior to the field tests, we conducted a validation of the RSSI levels provided by *libpcap* in a controlled lab environment using a cable connection between transmitter and receiver, adjustable attenuators and a spectrum analyzer. As a result, we concluded that the RSSI values presented by *libpcap* reflect the real received power (in dBm) almost satisfactorily, but contain a bias of approximately -3 dB for RSSI levels greater than -80 dBm and approximately -6 dB for RSSI levels smaller than -80 dBm. This means that the real received power is generally underestimated by the *libpcap* RSSIs. We therefore corrected the field test RSSI results accordingly to calculate the actual received power P_r.

In order to ensure statistical validity of the results, we performed at least 5 measurement runs per scenario, driving at low speeds (20-25 km/h) to collect as many samples per run as possible. We evaluated RSSI and PDR results for the scenarios described in section II-B which are plotted against the distance d_{RX} between the receiving vehicle and the center of the intersection. During the approaching phase of the receiver, negative values of d_{RX} are used for presentation purposes. For both performance metrics, we calculate means over 2.5 m distance intervals and include 95 % confidence intervals in the resulting plots. However, RSSI data is only collected for frames that were correctly received. For this reason, the measured mean received power levels overestimate the real mean levels of all frames significantly for low PDRs, but reflect real mean levels sufficiently well for high PDRs.

A. Intersection 1: Varying transmitter positions

The resulting mean received power $\bar{P}_r$ for varying transmitter positions at intersection 1 is shown in Fig. 4. As expected, the transmitter distance d_{TX} has a significant influence on the received power levels. Furthermore, there is a rapid increase before LOS conditions are available (LOS is only available approximately 10 m ahead of and behind the intersection), which suggests that, although this is a half-open intersection, lower order reflections significantly contribute to the received power. Fig. 5 depicts the mean PDR for varying transmitter

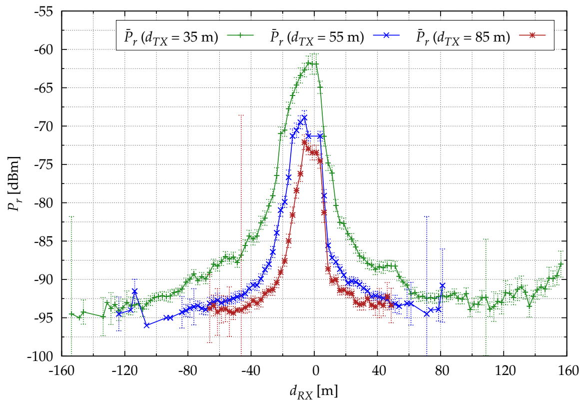

Figure 4: Mean received power $\bar{P}_r$ for varying distances d_{TX} between transmitter and intersection 1.

positions at intersection 1. It is clearly visible that the edges of the PDR plot are relatively steep, indicating a quick transition from unreliable to reliable communication performance and vice versa. For $d_{TX} = \{35, 55, 85\}$ m, fully reliable communication (PDR ≥ 0.9) is possible during the approaching phase for $d_{RX} \approx \{65, 30, 20\}$ m, respectively. For $d_{TX} = 35$ m and $d_{RX} \approx 90$ m, the influence of a gap between the buildings in the side street (see Fig. 3a) is evident.

B. Intersections 2 and 3: Varying street width

Figures 6a and 6b show mean PDRs and mean received power levels as well as the raw received power levels indicating the signal fading for the medium-wide side street at intersection 2 and the narrow side street at intersection 3. Although the transmitter's distance to the intersection was the same in both scenarios and the development of the surrounding buildings is very similar, the communication performance is considerably different. For the narrow side street, a PDR higher than 0.9 is achieved approximately 60 m ahead of the

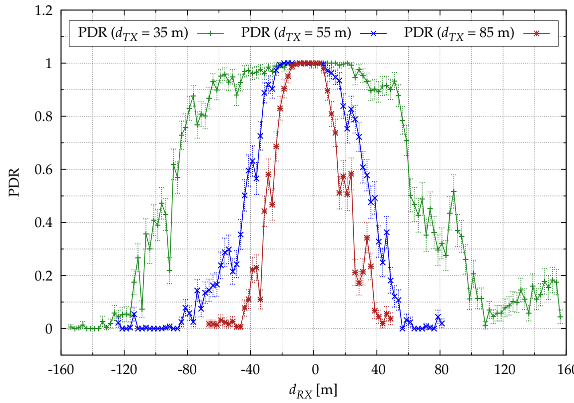

Figure 5: Mean PDRs for varying distances d_{TX} between transmitter and intersection 1.

intersection center. On the contrary, the same PDR is observed approximately 90 m ahead of the intersection center for the medium-wide side street. Regarding a distance $d_{TX} = 25$ m of the static transmitter to the intersection center in both scenarios, effective reliable communication ranges $d_{\text{eff}} = d_{RX} + d_{TX}$ of 85 m and 115 m, respectively, can be achieved.

Obviously, the opening width of an urban canyon has a significant impact on the maximum communication range. As diffraction is negligible at 5.9 GHz, a reasonable explanation for this effect might be reflexions of first and higher orders that reach the receiver earlier in a wider canyon. However, this phenomenon requires a deeper analysis in the future. Likewise, the effects of vegetation, which did not substantially influence the results in these scenarios, will be subject of further studies.

Despite differences concerning intersection topology and measurement setup, the results for intersection 2 are well in line with those for intersection 10 ("urban main case") in [8], which shows a similar, albeit not fully identical topology.

C. Intersection 4: Wide intersection with dense traffic

The results from the last scenario are shown in Fig. 6c. Although the intersection is relatively wide, the communication performance is worse than at intersection 2. Reliable communication (PDR ≥ 0.9) is only possible approximately 50 m ahead of the intersection center, which results, considering $d_{TX} = 45$ m, in an effective reliable communication range of $d_{\text{eff}} = d_{RX} + d_{TX} = 95$ m. This behavior might be caused by the influence of surrounding cars and especially buses on the propagation of the radio signal, which can be regarded as a kind of probabilistic shadowing. This could also cause the relatively gentle slope of the PDR plot.

IV. Conclusion

This paper presents the results of a 5.9 GHz V2V measurement campaign at urban intersections under NLOS conditions using commercial off-the-shelf wireless interface cards which meet the 802.11p and ITS-G5 specifications using a modified device driver. We evaluated received power levels and packet delivery ratios under varying conditions with respect to vehicle positioning, intersection geometry and traffic density.

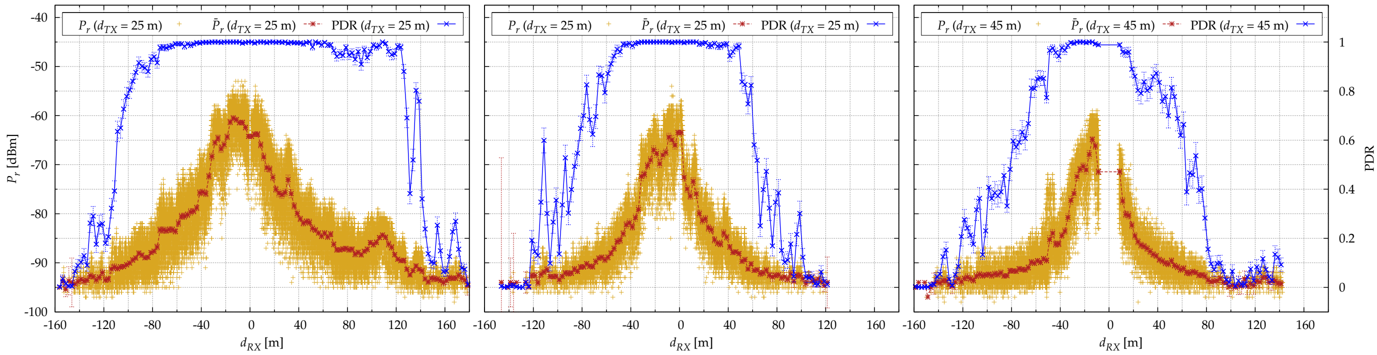

(a) Intersection 2: Medium-wide side street. (b) Intersection 3: Narrow side street. (c) Intersection 4: Wide intersection, dense traffic.

Figure 6: Raw received power (P_r), mean received power ($\bar{P}_r$) and mean PDR for intersections 2-4.

The achieved effective reliable communication ranges, calculated as sum of transmitter and receiver distances to the intersection center, were found to be between 85 m and 115 m for the selected intersections. Knowing the effective reliable communication range and the speed of the vehicles (e. g. 50 km/h), the *earliest reliable notification time* can easily be deduced assuming equal distances to the intersection for both vehicles threatened by a collision, which corresponds to a time to collision (TTC) between 3.1 s and 4.1 s.

Additionally, based on maximum decelerations and 1 s driver reaction time, stopping distances for dry asphalt, wet asphalt and a snow-covered road can be estimated as 26 m, 30 m and 63 m, respectively, at a speed of 50 km/h. In combination with the effective reliable communication ranges at the investigated intersections, this indicates that a collision avoidance application could work successfully with the exception of the snow-covered road, however, lower speeds seem to be more adequate in this special case, anyway.

Our results show that the width of the intersecting streets significantly affects communication performance and that traffic density seems to have an influence that cannot easily be neglected. Several observed effects related to urban radio propagation need a deeper analysis in future work. For this purpose, it is envisaged to deterministically model the channel for the investigated scenarios in combination with a PHY layer simulation.

Furthermore, scalability aspects of urban vehicular networks which suffer from frame collisions have to be analyzed using network simulations. In this context, the presented results are supposed to ease the development of urban V2V propagation models which have to consider buildings and other obstacles.

Acknowledgment

The authors are grateful to the Ministry of Science and Culture of Lower Saxony for funding our work within the Connected Cars in a Connected World (C3World) project. Furthermore, we thank Oleksandr Demchenko, Andreas Kwoczek and Delphi Deutschland GmbH for their valuable support.

References

[1] *Wireless LAN Medium Access Control (MAC) and Physical Layer (PHY) Specifications - Amendment 6: Wireless Access in Vehicular Environments*. IEEE 802.11p-2010.

[2] *Wireless LAN Medium Access Control (MAC) and Physical Layer (PHY) Specifications*. IEEE 802.11-2007.

[3] *Intelligent Transport Systems (ITS); European Profile Standard for the Physical and Medium Access Control Layer of Intelligent Transport Systems Operating in the 5 GHz Frequency Band*. ETSI ES 202 663 V1.1.0, 2010.

[4] A. F. Molisch, F. Tufvesson, J. Karedal, and C. Mecklenbrauker, “A Survey on Vehicle-to-Vehicle Propagation Channels,” *IEEE Wireless Communications*, vol. 16, no. 6, pp. 12–22, Dec. 2009.

[5] A. Paier, L. Bernado, J. Karedal, O. Klemp, and A. Kwoczek, “Overview of Vehicle-to-Vehicle Radio Channel Measurements for Collision Avoidance Applications,” in *IEEE 71st Vehicular Technology Conference*, 2010, pp. 1–5.

[6] M. Schack, J. Nuckelt, R. Geise, L. Thiele, and T. Kürner, “Comparison of Path Loss Measurements and Predictions at Urban Crossroads for C2C Communications,” in *Proceedings of the 5th European Conference on Antennas and Propagation (EUCAP)*, Apr. 2011, pp. 2896 – 2900.

[7] J. Karedal, F. Tufvesson, T. Abbas, O. Klemp, A. Paier, L. Bernado, and A. F. Molisch, “Radio Channel Measurements at Street Intersections for Vehicle-to-Vehicle Safety Applications,” in *2010 IEEE 71st Vehicular Technology Conference*, 2010, pp. 1–5.

[8] T. Mangel, M. Michl, O. Klemp, and H. Hartenstein, “Real-World Measurements of Non-Line-Of-Sight Reception Quality for 5.9GHz IEEE 802.11p at Intersections,” in *3rd Int. Workshop on Communication Technologies for Vehicles (Nets4Cars), LNCS, Vol. 6596*, 2011, pp. 189–202.

[9] A. Kwoczek, Z. Raida, J. Lacik, M. Pokorny, J. Puskely, J. Puskely, and P. Vagner, “Influence of Car Panorama Glass Roofs on Car2Car Communication,” in *2011 IEEE Vehicular Networking Conference (VNC)*. IEEE, Nov. 2011, pp. 246–251.